Supramolecular Chemistry

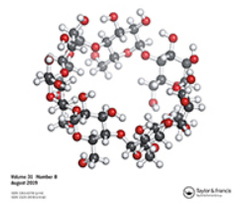

ISSN: 1061-0278 (Print) 1029-0478 (Online) Journal homepage: https://www.tandfonline.com/loi/gsch20

Oxidant aggregate-induced porosity in vapour-deposited polymer films and correlated impact on electrochemical properties

Wesley Viola, Lushuai Zhang & Trisha L. Andrew

To cite this article: Wesley Viola, Lushuai Zhang & Trisha L. Andrew (2019) Oxidant aggregate-induced porosity in vapour-deposited polymer films and correlated impact on electrochemical properties, Supramolecular Chemistry, 31:8, 491-498, DOI: 10.1080/10610278.2019.1623892

To link to this article: https://doi.org/10.1080/10610278.2019.1623892

Published online: 31 May 2019.

SUPRAMOLECULAR CHEMISTRY
2019, VOL. 31, NO. 8, 491–498
https://doi.org/10.1080/10610278.2019.1623892

Taylor & Francis
Taylor & Francis Group

ARTICLE

Oxidant aggregate-induced porosity in vapour-deposited polymer films and correlated impact on electrochemical properties

Wesley Viola[a], Lushuai Zhang[b,c] and Trisha L. Andrew[a,b]

[a]Department of Chemical Engineering, University of Massachusetts Amherst, Amherst, MA, USA; [b]Department of Chemistry, University of Massachusetts Amherst, Amherst, MA, USA; [c]Department of Biological Engineering, Massachusetts Institute of Technology, Cambridge, MA, USA

ABSTRACT

Persistently doped conjugated polymers are integral for energy storage, flexible electronics, and biosensors due to their unique ability to interact with both ionic and electronic currents. To maximise the performance of devices across these fields, research has focused on controlling material properties to optimise conductivities of both types of charge carriers. The challenge lies in improving ionic transport, which is typically the rate-limiting step in redox processes, without sacrificing electronic conductivity or desirable mechanical properties. Here we report on control of nanostructure in vapour deposited conducting polymer films and correlate changes in film structure with resulting electrochemical properties. Structural control is enabled by exploiting the growth of oxidant nanoaggregates during the reactive vapour deposition process. Relative to dense films, porous films exhibit faster response times in electrochemical testing. Scan rate analysis confirms a transition away from diffusion-limited charging kinetics and demonstrates the important role that porosity can play in ion transport through electroactive polymers. Advantageously, continuous polymer networks remain evident in nanostructured films, ensuring that high electronic conductivities are maintained along with high porosity. We find that such enhanced properties are retained even as polymer thickness increases ten-fold. The films reported herein may serve as robust electrodes in flexible electrochemical devices.

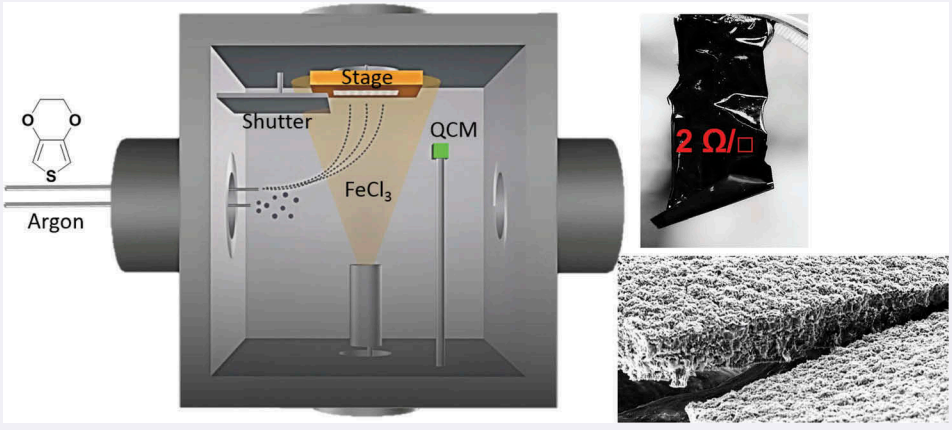

ARTICLE HISTORY
Received 28 February 2019
Accepted 22 May 2019

KEYWORDS
Conducting polymer; reactive vapor deposition; electrochemistry; porosity; aggregate

Introduction

Electrochemical processes are at the heart of many intensively researched, next-generation technologies. Energy storage, in the form of batteries, fuel cells, and capacitors, represents the oldest and most obvious application of electrochemistry, still commanding widespread interest both as a means of ending the dependence on fossil fuels and of enabling device innovations, especially in the field of wearable electronics. No longer simply a tool for energy storage, electroactive materials are now being developed for a multitude of applications, including polymeric actuators (1), desalination membranes (2), and organic electrochemical transistors (OECTs) (3). In bioelectronics, these materials have proved invaluable as they can interface between the ionic currents used in biological signalling pathways and the electronic currents present within the metals and semiconductors of devices (4).

A perennial problem posed to redox processes is the disparate transport mechanisms of ionic and electronic

CONTACT Trisha L. Andrew tandrew@umass.edu Department of Chemical Engineering, University of Massachusetts Amherst, Amherst, MA, USA

charge carriers (5). Whereas ionic species can be considered as classical particles obeying Fickian diffusion, electrons and holes are quantum particles that transport via band conduction and/or hopping. Generally, material properties which favour one transport mode inhibit the other, potentially leading to mismatched conductivities and impeded operation of the electrode processes described above (6). Careful material design is therefore needed to optimise for both modes of transport. In organic electronic materials, cosolvents have been used in formulations of poly(3,4-ethylenedioxythiophene):poly(styrene sulfonate) (PEDOT:PSS) to affect film morphology and improve ionic conductivity, though this comes at the expense of electronic conductivity (6). Other efforts have focused on tailoring the ionic species to facilitate solvation within the lamellar stacked morphology of polymers like poly(3-hexylthiophene) (P3HT) (7). The processing of carbon-based electrochemical materials often includes an exfoliation step to break pi-pi stacking among graphene units (8, 9).

Another common approach is extension of the electrode–electrolyte interface by introducing nano/microstructure throughout the bulk of the material. This is crucial in applications that demand high active mass loadings, where ion transport limitations are at their greatest. Many previously reported examples of nanostructured conjugated polymers are composed of loosely interconnected, discrete polymer units that may not be suitable for flexible energy storage devices. These include electrospun polyaniline nanofiber 'mats' (10), emulsion-polymerised hollow polypyrrole microspheres (11), and vapour-phase polymerised nanofibrillar PEDOT-X films (12). Gleason et al. reported on porous oxidative chemical vapour deposition (oCVD) PEDOT-Cl deposited using a $CuCl_2$ oxidant, though these films suffered from low conductivities and were not electrochemically characterised (13). Other efforts have been directed at conformally coating thin polymer films onto porous substrates such as carbon-based materials and nylon membranes (14, 15).

Here we report on control of intrinsic porosity of reactive vapour deposited PEDOT-X films and correlate nanostructure to electrochemical properties. Reactive vapour deposition (RVD) has been shown to produce robust, conformal films on arbitrarily rough substrates that can serve as textile electrodes for wearable electronics (16–19). Persistently *p*-doped PEDOT-X deposited in this fashion is an electrochemically active mixed electron and ion transporter. The metal-containing oxidant species typically used in RVD processes represent a handle by which to control polymer structure via nano-aggregation of excess oxidant crystals. In vapour-phase polymerisation (VPP), it has been shown that controlled hydrolysis of oxidant species can direct the growth of various PEDOT core-shell structures (20). Here we show that, by controlling process parameters in an oCVD deposition, namely the ratio of monomer to oxidant, we can direct assembly of oxidant nanoaggregates that embed within the polymer film during vapour deposition. A post-deposition rinse removes these salts, leaving behind a nanoporous, yet continuous polymer film that is highly suitable for electrochemical applications.

Materials and methods

Film Preparation. Films of persistently *p*-doped poly (3,4-ethylenedioxythiophene) (PEDOT-X) were directly deposited on 25 µm-thick polyimide films via oCVD, using a previously described reaction chamber and process parameters (16) (Figure 1). Briefly, 3,4-ethylenedioxythiophene (EDOT) (95%, TCI America) was used as the monomer and iron (III) chloride ($FeCl_3$) (97%, Sigma Aldrich) was used as the oxidant. EDOT was heated to 90°C and was delivered into chamber through a Swagelok SS-4JB needle valve. The needle valve was open for a quarter turn. Typically, the oxidant flux was 1.5 times higher than the monomer flux. A significantly lower monomer rate resulted in a non-uniform film over a 5 × 5 $inch^2$ substrate, while a significantly higher monomer rate sacrificed the conductivity of the resulting PEDOT-X film. Argon gas was used to maintain the total pressure in the chamber of 300 ± 10 mTorr and the substrate stage temperature was strictly maintained at 150°C during deposition.

Film deposition rate and the thickness were controlled by $FeCl_3$ evaporation rate, which was monitored by a quartz crystal microbalance (QCM) sensor located inside the chamber. Both the flow rate of the EDOT monomer and the oxidant contributed to the QCM reading. Due to the different positioning of the QCM relative to the substrate stage, the film growth rate at these surfaces is not equivalent but proportional by some factor. The ratio of the actual film thickness measured post-deposition to the real-time QCM reading during deposition was recorded as this 'tooling factor', which was found to be 0.5. QCM thickness readings were then corrected by this factor. The actual film growth rate was kept at 2 nm/s. As the desired film thickness was reached, the vacuum was maintained until the substrate stage was cooled below 60°C. Because of the iron (III) chloride oxidant used, chloride counterions were present in the as-deposited films, which likely underwent anion exchange upon rinsing. The as-deposited films were immersed in either 0.5 M H_2SO_4 or HCl for 15 min to remove trapped iron salts and other reaction by-products, as previously established (21). Films

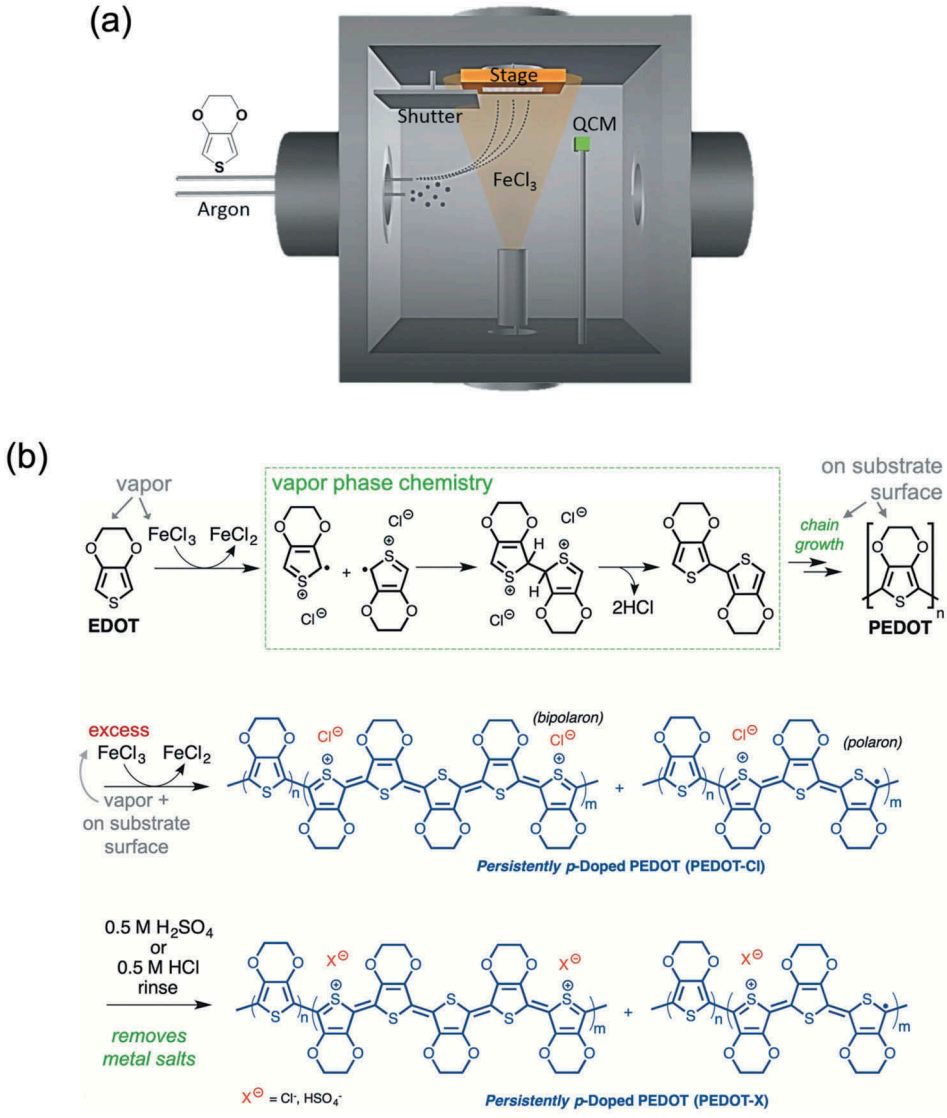

Figure 1. Reactive vapour deposition of persistently doped polymer films. a, Illustration of reactive vapour deposition chamber. b, Vapour phase chemistry and structure of doped conducting polymer film. Iron (III) chloride serves to both polymerise EDOT and to oxidise PEDOT (supplying a chloride counterion), forming persistently *p*-doped PEDOT-Cl. An acid rinse removes metal salts and results in counterion exchange to an ill-defined extent.

obtained u2sing this method remained *p*-doped even after rinsing/drying. Polymer films rinsed with HCl retained a chloride counterion after rinsing and are referred to as PEDOT-Cl. Polymer films rinsed with H_2SO_4 contained an ill-defined mixture of chloride, sulfate, hydrogen sulfate counterions and are referred to as PEDOT-X.

Free-standing films were obtained by vapour-depositing onto poly(tetrafluoroethylene) (PTFE) substrates, carefully peeling off the resulting monolithic films from the PTFE and immersing in 0.5 M H_2SO_4 for 15 min to rinse out residual iron salts.

Morphologically uniform 10 µm thick films could be created on a variety of substrates over a total lateral area of up to 10 cm × 10 cm (limited by the size of the substrate stage). The maximum film thickness reported here, 10 µm, is not determined by an innate material or process characteristic but, rather, by the practical fill capacity of the electrical furnace used in our chamber to vaporise $FeCl_3$. Use of a larger furnace with higher fill capacity should allow access to thicker films.

Electrochemical Analysis of Vapour-Deposited PEDOT-X. The volumetric capacitance was characterised by three-electrode cyclic voltammetry measurements by using a Wavenow potentiostat from Pine Instruments. A platinum wire was used as the counter electrode, Ag/AgCl in 1 M KCl as the reference electrode, and 0.5 M aqueous H_2SO_4 as the electrolyte.

Calculations. The volumetric capacitances of PEDOT-X electrodes were calculated from three-electrode CV measurements using Equation 1.

$$C_{electrode} = \frac{\int jdV}{2v\Delta V} \cdot \left[F/cm^3\right] \quad (1)$$

where j is current density normalised to the volume of PEDOT-X film, V is voltage, v is scan rate, ΔV is voltage window.

Results and discussion

The reactive vapour deposition of persistently *p*-doped poly(3,4 ethylenedioxythiophene) (PEDOT-X) is carried out in a custom-built reactor (Figure 1(a)) (16, 17). Vapour-phase oxidative polymerisation of the electron-rich monomer, 3,4-ethylenedioxythiophene (EDOT), effected by an iron (III) chloride oxidant yields *in situ* conducting polymer growth (Figure 1(b)). Process parameters such as chamber pressure, monomer/oxidant flux, substrate stage temperature, and deposition time can be actively tuned during deposition to optimise polymer molecular weight, film uniformity and electrical conductivity (17). Higher oxidant flux, relative to monomer flux, is typically employed to promote *p*-doping concomitantly with film formation.

Aggregates of the excess iron (III) chloride oxidant and iron (II) chloride by-products are uniformly dispersed throughout the bulk of the polymer film during growth. These aggregates are dissolved out of the film during a post-deposition acid rinse (18) in aqueous sulfuric acid (Figure 2), leaving behind empty 100–200 nm-sized nanopores. The simultaneous removal of elemental iron and appearance of a porous nanostructure can be seen in the EDX and SEM characterisations of the polymer film before and after rinsing. Since oxidant aggregates are uniformly dispersed throughout the bulk of the film, this nanostructure extends the full 10 μm thickness of the porous PEDOT-X films.

Polymer morphology may be controlled by adjusting the ratio of EDOT monomer to iron (III) chloride oxidant during the vapour deposition process. Real-time control of the reactant ratio, enabled by the chamber's internal QCM sensor, gives rise to dense polymer films at high relative monomer flux and very porous films at high oxidant flux. With a minimal loading of iron (III) chloride, the dense films lack nanostructure and, as expected, retain their morphology following rinsing.

In electrochemical applications, the morphology of active electrode materials plays a significant role in the kinetics of redox-driven charging. The ability to tune the nanostructure of our PEDOT-X films allows for optimisation of this process, as porous channels efficiently shuttle ions through the bulk. Electrochemical characterisations of the dense and porous films demonstrate this interdependence between film morphology and electrochemical performance (Figure 3). Using a three-electrode cyclic voltammetry, we show the dense PEDOT-Cl film shows sluggish charging kinetics as the infiltration of ions is impeded, while the porous film

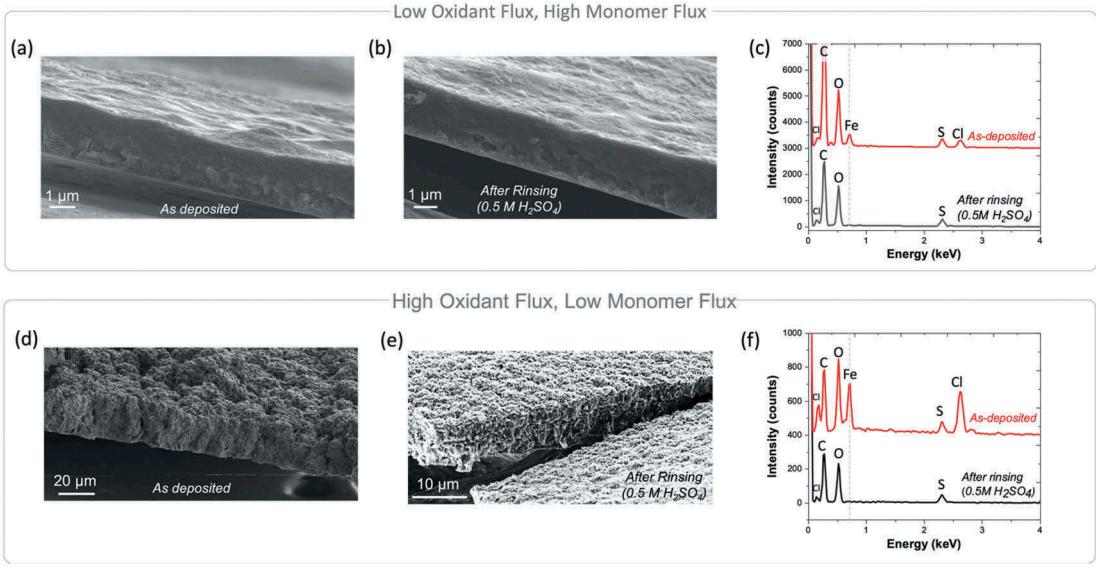

Figure 2. Controlled porosity in vapour deposited PEDOT-X. a-c, Films deposited at low oxidant flux and high monomer flux. Cross-section scanning electron micrographs (SEMs) of as-deposited (a) and acid rinsed (b) films with corresponding energy dispersive X-ray (EDX) spectra (c) showing removal of iron residues. d-f Films deposited at high oxidant flux and low monomer flux. Cross-section SEMs of as-deposited (d) and acid rinsed (e) films with resulting porous morphology and corresponding EDX spectra (f) showing removal of iron residues.

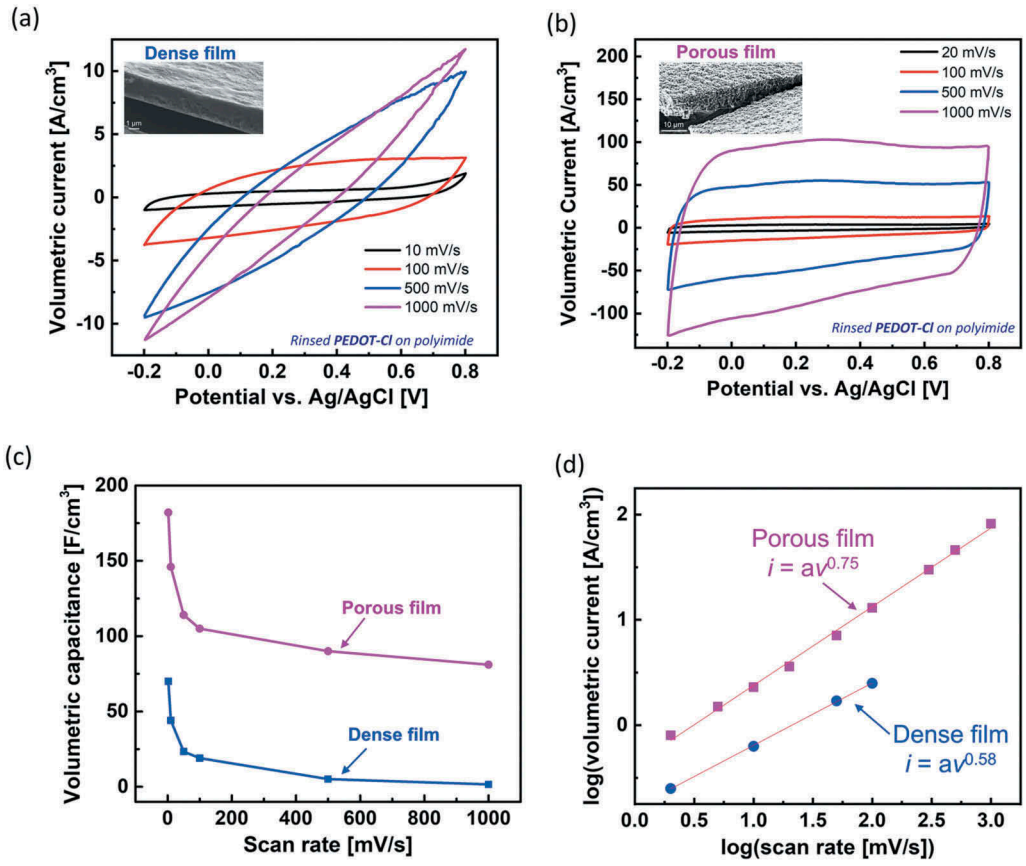

Figure 3. Electrochemical correlation to changes in film porosity. a,b, Three-electrode cyclic voltammetry of dense (a) and porous (b) PEDOT-Cl films (after acid rinsing). c,d Scan rate dependence of volumetric capacitance of porous and dense films. Log-log plot (d) with labelled i–v relationships.

maintains highly rectangular profiles even at rates of 1000 mV/s.

Further analysis of the charging kinetics may be done by examining the relationship between electrochemical current and scan rate (Figure 3(c)). Log-log plots of this data show that for dense films, current closely scales with the square root of the scan rate ($i \sim v^{0.58}$), indicative of diffusion-limited kinetics (Figure 3(d)) (22). With the introduction of porous channels that facilitate ion diffusion, the charging current of the porous films is closer to being directly proportional to scan rate ($i \sim v^{\infty 0.75}$), indicating nearly full redox accessibility of the electroactive polymer film even at high charging rates.

The influence of mass loading on the volumetric capacitance of vapour-deposited, porous PEDOT-Cl films is investigated using three-electrode cyclic voltammetry in aqueous sulfuric acid electrolytes. In comparing among films of varying thickness, capacitance normalised by volume of the active layer is a more meaningful quantity since it is an intrinsic property that, in the absence of transport limitations, will be constant for varying material thicknesses (23). Volume-normalised cyclic voltammograms of 0.2 µm, 1 µm and 10 µm thick PEDOT-Cl films on polyimide are mostly similar to each other (Figure 4(a)), meaning that the porous, vapour deposited PEDOT-Cl films maintain their electrochemical behaviour even at high mass loadings. Calculated volumetric capacitance values (three-electrode setup) for 0.2 µm, 1 µm and 10 µm-thick films at a 2mV/s scan rate are 173 F/cm^3, 189 F/cm^3 and 182 F/cm^3, respectively. Similar volumetric capacitances are observed for thin versus thick PEDOT-Cl films even at high scan rates (Figure 4(b)), suggesting that both electron and ion transport is optimised in these films.

Electrical impedance spectroscopy performed in aqueous sulfuric acid electrolytes using two PEDOT-Cl-coated polyimide substrates as electrodes provides deeper insight into the internal resistances operating within the vapour-deposited film. Near-vertical lines are observed in Nyquist plots for PEDOT-Cl films of varying thickness, similar to a platinum electrode control (Figure 4(c)). A semicircle is not observed at high frequency, even for thick films, confirming minimal charge exchange resistance and efficient ion diffusion in 10 µm thick vapour-deposited PEDOT-Cl. Impedance phase angle analysis (Bode plot, Figure 4(d)) also

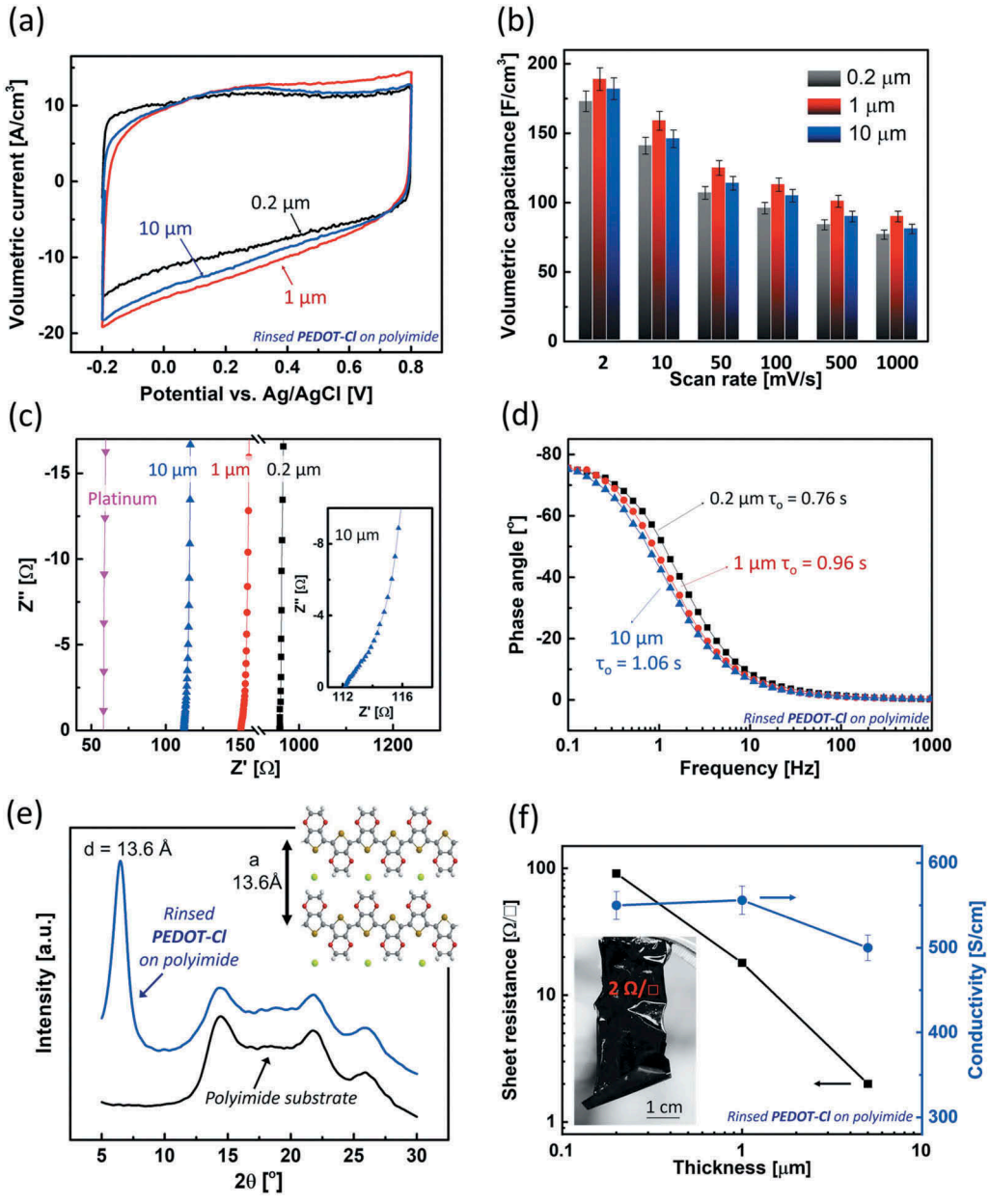

Figure 4. Porous PEDOT-Cl thickness study. a, Three-electrode cyclic voltammograms of 0.2 µm, 1 µm and 10 µm-thick porous PEDOT-Cl films on polyimide in 0.5 M H2SO4 aqueous electrolyte at scan rate of 100 mV/s with current normalised to volume of film. b, Scan rate dependence of volumetric capacitance of 0.2 µm, 1 µm and 10 µm-thick PEDOT-Cl films (three-electrode measurement). c, Nyquist plots of the impedance of symmetric PEDOT-Cl electrodes, in comparison to platinum electrodes. Inset: magnification for the high-frequency region for 10 µm-thick PEDOT-Cl. d, Impedance phase angle versus frequency for symmetric PEDOT-Cl electrodes of varying thickness. e, X-ray diffraction spectrum of a 10 µm-thick PEDOT-Cl film deposited on polyimide. f, Sheet resistance and conductivity of PEDOT-Cl films of varying thickness.

reveals similar ion transport impedances for thin and thick electrodes. The corresponding time constants (read from the inverse of the characteristic frequency at which −45° is reached) are similar for PEDOT-Cl electrodes of different thicknesses, confirming efficient ion transport through the polymer bulk. This series of experiments prove that thick, vapour-deposited PEDOT-Cl films act as high-performance electrochemical electrodes without the need for a metal charge collector.

The X-ray diffraction (XRD) spectrum (Figure 4(e)) of a 10 µm thick porous PEDOT-Cl film on polyimide shows a sharp diffraction peak at 2θ = 6.48. The corresponding d value of 13.6 Å matches the (100) axis of crystalline PEDOT-Cl (24), revealing the lamellar packing of PEDOT-Cl chains normal to the surface, even in highly porous films. Charge transport should be maximised within crystalline domains (25) and, therefore, these PEDOT-Cl films are expected to display high electronic conductivities.

Indeed, the sheet resistance of porous PEDOT-Cl films on polyimide linearly decreases from 91 to 2 Ω/square with increasing film thickness (Figure 4(f)). High conductivities above 500 S/cm are maintained even as film thicknesses are increased from 0.2 to 10 μm. Such high conductivity values confirm that thick, porous films nonetheless retain continuous polymer networks, ensuring that high electronic conductivities are maintained along with high porosity.

In sum, the combined presence of crystalline PEDOT-Cl domains (that promote charge transport) and uniformly distributed nanopores throughout the polymer bulk (that promote electrolyte penetration and ion transport deep within the film) result in concomitant optimisation of both ionic and electronic charge carriers, despite their disparate transport mechanisms. This claim is confirmed by the nearly rectangular cyclic voltammograms observed for 10 μm thick PEDOT-Cl films on polyimide at a high scan rate of 1 V/s.

Conclusions

Reactive vapour deposition creates thick films of electroactive conjugated polymers that are highly conductive and can act as sole-component electrodes for electrochemical charge storage devices. The unique, porous-yet-crystalline film structure created by a combined reactive vapour deposition/acid rinse sequence is critical for enabling efficient charge and ion transport in electroactive materials. Here we demonstrate tunable control of this nanostructure and correlate it to electrochemical properties of the resulting films. Analogous to solution-processed nanocarbon and transition metal oxide/dichalcogenide electrodes, the nanoscale porosity in vapour deposited polymer films allows for increased polymer/electrolyte contact and rapid ion transport, leading to thickness independent volumetric capacitances, which is not a common feature of most conducting polymer-based electrode materials.

The results of this report are significant to all electrochemical applications of polymers, including energy storage, biosensors, OECTs, and desalination membranes. The real-time control of porosity demonstrated here also suggests the ability to introduce a porosity gradient by varying the oxidant flux over the course of the deposition. This may have implications in material design for certain electrochemical technologies, e.g. polymeric actuators, where gradient structures play an important role in modulating mechanical responses (1).

Further, design principles established by the supramolecular chemistry community can be exploited to exquisitely direct the size, shape and orientation of the pores within vapour-deposited polymer films. For example, by using well-defined and judiciously selected iron (III) complexes and/or clusters as the oxidant, one can direct the size, geometry and length of the oxidant aggregates that evolve during vapour deposition, which will eventually determine the nature of the pores left behind in the acid-rinsed polymer films. In this way, molecular self-organisation can be exploited to create hierarchical mesostructure in soft electronic materials. These strategies will be the focus of forthcoming publications from our lab.

Disclosure statement

No potential conflict of interest was reported by the authors.

Funding

The authors gratefully acknowledge partial financial support from the US Air Force Office of Scientific Research under Agreement number [FA9550-14-1-0128], and from the National Science Foundation, CBET Division, Award [1706633].

ORCID

Trisha L. Andrew http://orcid.org/0000-0002-8193-2912

References

(1) Qiu, X.; Dzubiella, J.; Huang, F.; Zhao, Q.; Heyda, J.; Zhang, Z.; Antonietti, M.; Dunlop, J.W.C.; Yuan, J. An Instant Multi-Responsive Porous Polymer Actuator Driven by Solvent Molecule Sorption. *Nat. Commun.* **2014**, *5*(1), 1–8. DOI: 10.1038/ncomms5293

(2) Anderson, M.A.; Cudero, A.L.; Palma, J. Capacitive Deionization as an Electrochemical Means of Saving Energy and Delivering Clean Water. Comparison to Present Desalination Practices: Will It Compete? *Electrochim. Acta*. **2010**, *55*(12), 3845–3856. DOI: 10.1016/j.electacta.2010.02.012

(3) Khodagholy, D.; Rivnay, J.; Sessolo, M.; Gurfinkel, M.; Leleux, P.; Jimison, L.H.; Stavrinidou, E.; Herve, T.; Sanaur, S.; Owens, R.M., et al. High Transconductance Organic Electrochemical Transistors. *Nat. Commun.* **2013**, *4*, 1–6. DOI: 10.1038/ncomms3133

(4) Sheliakina, M.; Mostert, A.B.; Meredith, P. Decoupling Ionicand Electronic Currents in Melanin. *Adv. Funct. Mater.* **2018**, *28*(46), 1–7. DOI: 10.1002/adfm.201805514

(5) Zhang, L.; Andrew, T.L. Deposition Dependent Ion Transport in Doped Conjugated Polymer Films : Insights for Creating High-Performance Electrochemical Devices. *Adv. Mater. Interfaces*. **2017**, *1700873*, 1–9. DOI: 10.1002/admi.201700873

(6) Rivnay, J.; Inal, S.; Collins, B.A.; Sessolo, M.; Stavrinidou, E.; Strakosas, X.; Tassone, C.; Delongchamp, D.M.; Malliaras, G.G. Structural Control of Mixed Ionic and Electronic Transport in Conducting Polymers. *Nat. Commun.* **2016**, *7*, 1–9. DOI: 10.1038/ncomms11287

(7) Flagg, L.Q.; Giridharagopal, R.; Guo, J.; Ginger, D.S. Anion-Dependent Doping and Charge Transport in Organic Electrochemical Transistors. *Chem. Mater.* **2018**, *30*(15), 5380–5389. DOI: 10.1021/acs.chemmater.8b02220

(8) Kleinhammes, A.; Piner, R.D.; Jia, Y.; Dikin, D.A.; Stankovich, S.; Nguyen, S.T.; Kohlhaas, K.A.; Ruoff, R.S.; Wu, Y. Synthesis of Graphene-Based Nanosheets via Chemical Reduction of Exfoliated Graphite Oxide. *Carbon N. Y.* **2007**, *45*(7), 1558–1565. DOI: 10.1016/j.carbon.2007.02.034

(9) Yang, Y.; Huang, Q.; Niu, L.; Wang, D.; Yan, C.; She, Y.; Zheng, Z. Waterproof, Ultrahigh Areal-Capacitance, Wearable Supercapacitor Fabrics. *Adv. Mater.* **2017**, *29* (19), DOI: 10.1002/adma.201606679

(10) Chaudhari, S.; Sharma, Y.; Archana, P.S.; Jose, R.; Ramakrishna, S.; Mhaisalkar, S.; Srinivasan, M. Electrospun Polyaniline Nanofibers Web Electrodes for Supercapacitors. *J. Appl. Polym. Sci.* **2013**, *129*(4), 1660–1668. DOI: 10.1002/app.38859

(11) Shi, Y.; Pan, L.; Liu, B.; Wang, Y.; Cui, Y.; Bao, Z.; Yu, G. Nanostructured Conductive Polypyrrole Hydrogels as High-Performance, Flexible Supercapacitor Electrodes. *J. Mater. Chem. A.* **2014**, *2*(17), 6086–6091. DOI: 10.1039/c4ta00484a

(12) D'Arcy, J.M.; El-Kady, M.F.; Khine, P.P.; Zhang, L.; Lee, S. H.; Davis, N.R.; Liu, D.S.; Yeung, M.T.; Kim, S.Y.; Turner, C. L., et al. Vapor-Phase Polymerization of Nanofibrillar Poly(3,4- Ethylenedioxythiophene) for Supercapacitors. *ACS Nano*. **2014**, *8* (2), 1500–1510. DOI: 10.1021/nn405595r

(13) Im, S.G.; Kusters, D.; Choi, W.; Baxamusa, S.H.; Van de Sanden, M.C.M.; Gleason, K.K. Conformal Coverage of Poly (3, 4-Ethylenedioxythiophene) Films with Tunable Nanoporosity via Oxidative Chemical Vapor Deposition. *ACS Nano*. **2008**, *2*(9), 1959–1967. DOI: 10.1021/nn800380e

(14) Nejati, S.; Minford, T.E.; Smolin, Y.Y.; Lau, K.K. Enhanced Charge Storage of Ultrathin Polythiophene Films within Porous Nanostructures. *ACS Nano*. **2014**, *8*(6), 5413–5422. DOI: 10.1021/nn500007c

(15) Arnold, S.P.; Harris, J.K.; Neelamraju, B.; Rudolph, M.; Ratcliff, E.L. Microstructure-Dependent Electrochemical Properties of Chemical-Vapor Deposited Poly (3, 4-Ethylenedioxythiophene)(Pedot) Films. *Synth. Met.* **2019**, *253* (26–33), 1.

(16) Zhang, L.; Fairbanks, M.; Andrew, T.L. Rugged Textile Electrodes for Wearable Devices Obtained by Vapor Coating Off-the-Shelf, Plain-Woven Fabrics. *Adv. Funct. Mater.* **2017**, *27*(24), 1–9. DOI: 10.1002/adfm.201700415

(17) Zhang, L.; Viola, W.; Andrew, T.L. High Energy Density, Super-Deformable, Garment-Integrated Microsupercapacitors for Powering Wearable Electronics. *ACS Appl. Mater. Interfaces*. **2018**, *10* (43), 36834–36840. DOI: 10.1021/acsami.8b08408

(18) Zhang, L.; Andrew, T.L. Using the Surface Features of Plant Matter to Create All-Polymer Pseudocapacitors with High Areal Capacitance. *ACS Appl. Mater. Interfaces*. **2018**, *10*, 38574–38580. DOI: 10.1021/acsami.8b12551

(19) Borrelli, D.C.; Ugur, A.; Gleason, K.K.; Jo, W.J.; Lee, S.; Chen, N.; Petruczok, C.D.; Wang, X.; Howden, R.M.; Coclite, A.M., et al. 25th Anniversary Article: CVD Polymers: A New Paradigm for Surface Modification and Device Fabrication. *Adv. Mater.* **2013**, *25* (38), 5392–5423. DOI: 10.1002/adma.201301878

(20) Wang, H.; Diao, Y.; Rubin, M.; Santino, L.M.; Lu, Y.; D'Arcy, J. M. Metal Oxide-Assisted PEDOT Nanostructures via Hydrolysis-Assisted Vapor-Phase Polymerization for Energy Storage. *ACS Appl. Nano Mater.* **2018**, *1*(3), 1219–1227. DOI: 10.1021/acsanm.7b00382

(21) Im, S.G.; Gleason, K.K.; Olivetti, E.A. Doping Level and Work Function Control in Oxidative Chemical Vapor Deposited Poly (3,4-Ethylenedioxythiophene). *Appl. Phys. Lett.* **2007**, *90*(15), 1–4. DOI: 10.1063/1.2721376

(22) Kaufman, D.; Hudson, K.L.; Mcclamrock, R. Where Do Batteries End and Supercapacitors Begin? *Sci. (80-.)*. **2014**, *343*(March), 1210–1211. DOI: 10.1126/science.1249625

(23) Meryl, D.S.; Ruoff, R.S. Best Practice Methods for Determining an Electrode Material's Performance for Ultracapacitors. *Energy Environ. Sci.* **2010**, *3*(9), 1294–1301. DOI: 10.1039/C0EE00074D

(24) Niu, L.; Kvarnström, C.; Fröberg, K.; Ivaska, A. Electrochemically Controlled Surface Morphology and Crystallinity in poly(3,4-Ethylenedioxythiophene) Films. *Synth. Met.* **2001**, *122*(2), 425–429. DOI: 10.1016/S0379-6779(00)00562-2

(25) Im, S.G.; Gleason, K.K. Systematic Control of the Electrical Conductivity of Poly(3,4-Ethylenedioxythiophene) via Oxidative Chemical Vapor Deposition. *Macromolecules*. **2007**, *40*(18), 6552–6556. DOI: 10.1021/ma0628477